LAWRENCE
LIVERMORE
NATIONAL
LABORATORY

LLNL-CONF-434285

Pillar structured thermal neutron detectors: effects of high radiation fluence

Q. Shao, A. M. Conway, R. Radev, L. F. Voss, T. F. Wang, C. L. Cheung, L. Fabris, R. J. Nikolic

June 7, 2010

INMM 51st Annual Meeting
Baltimore, MD, United States
July 11, 2010 through July 15, 2010

Disclaimer

PILLAR STRUCTURED THERMAL NEUTRON DETECTORS: EFFECTS OF RADIATION FLUENCE

[1]Q. Shao, [1]A. M. Conway, [1]R. Radev, [1]L. F. Voss, [1]T. F. Wang, [2]C. L. Cheung, [3]L. Fabris and [1,*]R. J. Nikolić
[1]Lawrence Livermore National Lab, [2]University of Nebraska-Lincoln, [3]Oak Ridge National Lab
*Corresponding author electronic mail: nikolic1@llnl.gov

ABSTRACT

Solid state thermal neutron detectors are desired to replace the current ^{3}He tube based technology, which has some issues with stability, sensitivity to microphonics and very recently a shortage in ^{3}He. There have been several solid state thermal neutron detector concepts developed recently. Our approach is based on the combination of high aspect ratio silicon PIN diodes surrounded by ^{10}B, the neutron converter material. Etching high aspect ratio pillar structures into silicon produces a device that can efficiently absorb the thermal neutrons because of a large volume of ^{10}B within the pillar array. The charged particles generated by the thermal neutron - ^{10}B reaction are detected in the PIN diodes by spacing the pillars to optimize reaction product collection efficiency. In this paper, preliminary results indicate that our device can withstand a certain amount of neutron and gamma fluence without deterioration of detector's performance.

INTRODUCTION

Neutron coincidence counting is one of the key safeguards measurements to determine nuclear material signatures. When combined with gamma-ray isotopic results, it will be able to determine the mass of the homogeneous special nuclear materials. The current neutron coincidence systems are all ^{3}He based counters. The shortage of ^{3}He has mandated the evaluation of alternative techniques. Many solid-state devices are being investigated. Our device is based on a high aspect ratio PIN diodes filled with ^{10}B which we have coined "Pillar Detector" [1-6]. To be able to construct large area detection systems to replace current ^{3}He tubes based systems, we will need to assemble arrays of solid state neutron detectors. This highly segmented system will be able to withstand significant higher neutron count rate as well as possible mapping of the location of neutron sources. Moreover, the system will be lighter and smaller than ^{3}He tubes, since it is basically constructed with thin layers of neutron detector arrays, thereby significantly improving the probability so that it may be used as an inspection tool. A comparison of the primary detector figures-of-merit for our device (after appropriate scaling) and ^{3}He tubes is shown in Figure 1.

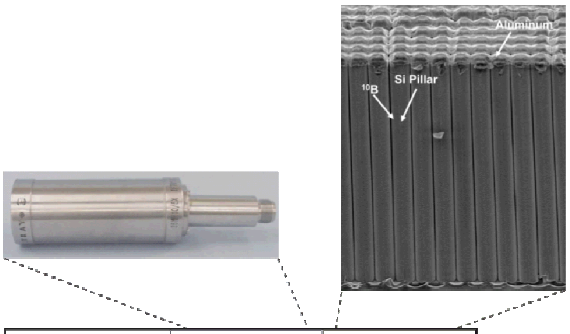

	^{3}He Tube	Pillar Detector
Efficiency	20–90%	50+%
Required voltage	1000 V	<10 V
Fieldability	Microphonics, HV, air transport	Rugged Not Commercial

Figure 1 Comparison of the primary detector figures-of-merit for pillar structured thermal neutron detector and ^{3}He tubes.

Thermal neutrons have a low probability of interacting with conventional semiconductor materials. Thus, a two step detection process is generally required. First, the thermal neutrons are converted to energetic ions by a material with a high thermal neutron cross-section. In our device ^{10}B is used (its cross-section for thermal neutrons is σ = 3,837 barns) resulting in the following reaction: n + ^{10}B → α + ^{7}Li. Second, these ions are collected using a reverse biased semiconductor diode. Three major criteria drive the optimal design of thermal neutron detectors: sufficient thickness of neutron convertor material (50 μm in ^{10}B), high probability of ion energy deposition within semiconductor detector (ion track length 3 μm in ^{10}B), and large discrimination between gamma ray events and thermal neutron events. Using a three-dimensionally integrated approach, very high detection efficiency is possible because the geometrical constraints on the converter material thickness are decoupled from the limitation of the ion track length, as shown in Figure 2. In this case, the ^{10}B thickness is defined by the pillar height (etch depth) so as to absorb the thermal neutrons. The pillar pitch is defined lithographically to allow the highest possible interaction of the energetic ions with the semiconductor pillars. Our highest efficiency of 20% to date has been achieved with an array of etched Si pillars with 13:1 aspect ratio (2x2 μm^2 pillars with a 26 μm etch depth or height and a separation of 2 μm) on a planar silicon substrate, arranged in a square matrix. When the 3D Pillar Detector is scaled to 50+ μm, a high efficiency device (> 50%) is predicted [1-4, 6].

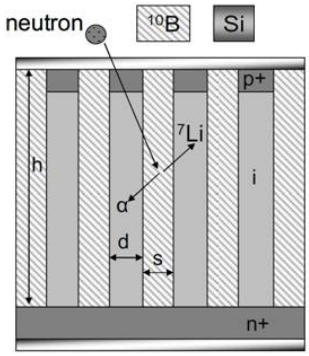

Figure 2 Schematic of a pillar structured thermal neutron detector. h: pillar height (26 μm), d: pillar size (2 μm), s: pillar separation (2 μm).

An electrically stable, mechanically robust, and radiation hard detector is needed for safeguard applications, which requires operation in high radiation environments. Radiation damage is generally caused by the collision of an energetic particle or photon with an atom. This can result in the atom being displaced to an interstitial position or electronic charge displacement [7-8]. The nature of the perturbation to the crystal lattice and mechanism of modified charge transport is complicated. A simplistic view is that high fluence radiation creates defects or generation centers in the bulk depletion regions of reverse biased diodes. In Shockley-Read-Hall theory of generation-recombination [9], electron and holes are generated via the generation centers, and they are swept out of the space region by the electric field to form a generation current. For most silicon devices, this generation process dominates in producing dark current [10]. In fact, reports of the leakage current increase in high resistivity silicon CCDs shows an excess dark current over that of Shockley-Read-Hall theory of generation-recombination in which the defect levels in the bandgap are regarded as acting independently of each other. Watts et al reported the irradiation causes an intercenter charge transfer [11]. In the theory of intercenter charge transfer, several defect energy levels created in the bandgap by radiation act as coupled generation centers since defects are in close proximity to each other. An electron is first captured by a donor state close to the top of valence band. The electron can then transfer directly to a higher state in a nearby defect without going via the conduction band. The enhancement of the generation rate arises because the presence of donor level increases the transition probability from valence band to the above midgap level greatly [12-14]. Clearly the defects introduced by radiation affect the performance of the detector because they may act as trapping centers for charge carriers or they may create fixed charge complexes which in some circumstances can be removed by thermal annealing. Additional trapping centers and new energy states change the charge collection efficiency, leakage current, capacitance, pulse risetime, and other properties of neutron detectors.

In this paper, the effect of radiation fluence with gamma-rays and neutrons on 3D pillar structured thermal neutron detector has been studied. The evaluation of our pillar structured detector is carefully evaluated against a flat silicon detector to determine if there are additional failure modalities due to the large surface area of the pillars. A second control sample involving pillars but without boron is also included to evaluate the robustness of the boron within the pillars.

EXPERIMENTAL

Three devices were studied in this work: a planar PIN diode designated F1, a pillar structured PIN diode filled with photoresist designated P1 and pillar structured PIN diode filled with ^{10}B designated D1. All of them are p^+-n^--n^+ in structure with a doping concentration of 3×10^{13} cm^{-3} in the n^- region. The physical sizes for them are 25 mm^2, 2.2 mm^2 and 9 mm^2 respectively. The pillar diameter and spacing is defined lithographically, followed by plasma etching to create high aspect ratio structures as shown in Figure 3 (a). The pillar platform is then either filled with ^{10}B by low pressure chemical vapor deposition (D1) as shown in Figure 3 (b) or spin-coated photoresist (P1). The excess Boron or photoresist are etched away by plasma etching to expose the top of pillars for metallization as shown in Figure 3 (c).

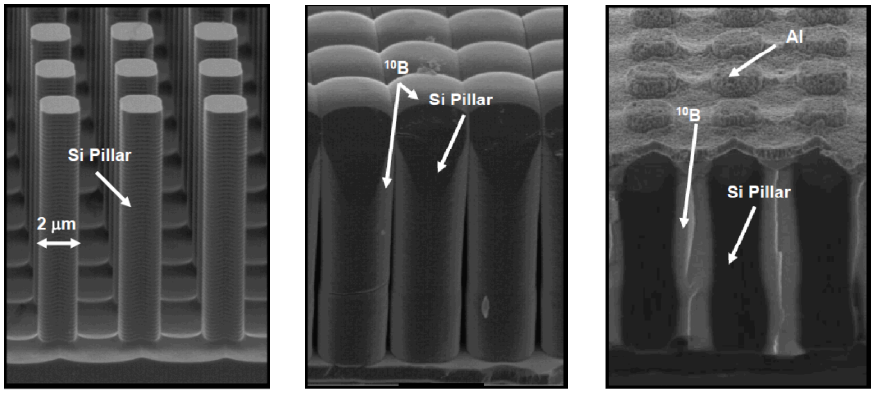

(a) (b) (c)

Figure 3 Scanning electron microscopy images of 26 μm silicon pillars structures: (a) as fabricated by etching, (b) after boron deposition, and (c) after etch-back of excess boron and aluminum evaporation.

Three devices, F1, P1 and D1 were irradiated with two ^{137}Cs gamma sources with activities of 6.45×10^5 MBq (17.4 Ci) and 8.76×10^6 MBq (236.8 Ci) as shown in Figure 4 (a, b). For detector D1, the corresponding gamma (photon) fluence rates at the points of measurement were 4.37×10^8 photons/(cm^2·sec) and 2.64×10^9 photons/(cm^2·sec) respectively. For F1 and P1, the corresponding gamma (photon) fluence rates at the points of measurement were 2.59×10^8 photons/(cm^2·sec) and 2.64×10^9 photons/(cm^2·sec) respectively. The devices were exposed to the ^{137}Cs source with the lower activity for 100,000 seconds and the one with higher activity for 60,000 seconds. The total gamma fluence delivered was 2.0×10^{14} photons/cm^2 for D1 and 1.84×10^{14} photons/cm^2 for F1 and P1. In order to investigate the neutron radiation hardness of our detector, D1 was then exposed to a neutron fluence rate of 3.2×10^3 n/(cm^2·sec) from a bare (free-in-air) ^{252}Cf neutron source for 60,000 seconds as shown in Figure 4(c). The total neutron fluence delivered was 1.9×10^8 n/cm^2.

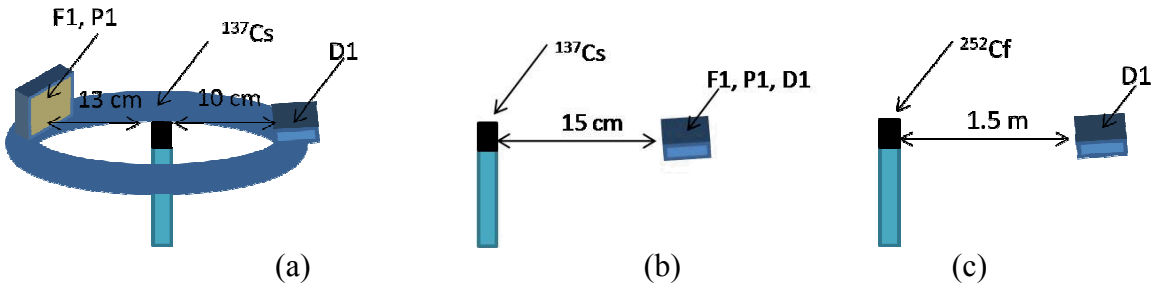

Figure 4 Experimental setups of gamma irradiation (a, b) and fast neutron irradiation (c).

RESULTS AND DISCUSSION

1. Device performance after gamma irradiation

Current-voltage (I-V), capacitance-voltage (C-V), and open-circuit voltage decay (OCVD) measurements were taken on all three devices prior to exposure, after 100,000 seconds of exposure to the lower activity gamma source, and after 60,000 seconds of exposure to the higher activity gamma source. Figure 5 shows the current-voltage characteristics of three devices. All devices were biased up to -10 V. The leakage current is inversely proportional to the generation lifetime, which is related to the density of trapping centers in the depletion region. There is no noticeable increase in the leakage current after irradiation, indicating little damage was introduced by the gamma irradiation. Effective carrier lifetimes were monitored by using OCVD [15-17]. In this method, a diode is forward biased to achieve a steady-state excess carrier concentration in a lightly doped region. Subsequently the diode bias is removed (open circuit) to enable recombination of the excess carriers. The effective carrier lifetime is extracted from the slope of the voltage decay waveform. The effective lifetime is associated with bulk lifetime and surface recombination velocities [5]. As shown in Figure 6, the decay waveforms are exactly same for all three devices before and after the gamma irradiation. That demonstrates that there is no appreciable damage induced by the irradiation. The extracted effective lifetimes at low level injection, which means the injected minority carrier concentration is lower than the equilibrium majority carrier concentration [17], are 0.5 μs, 9.5 μs and 1.0 μs for F1, P1 and D1 respectively. Ideally, the effective lifetime of flat diode (F1) is longer than pillar diode (P1) and detector (D1) due to its smaller surface to area ratio. In this particular case, the active area of F1 is defined by saw-dicing and P1 and D1 are defined by plasma etching. The damage and contamination introduced by saw-dicing at sidewall surfaces serve as effective recombination centers via which the electron and hole recombine, so effective lifetime is dramatically shortened from its theoretical value (~ 30 μs). Figure 7 shows the comparison of capacitances of devices before and after gamma irradiation. Capacitance of a semiconductor PIN diode is related to the change of charge within the depletion region. The increase of device capacitance can decrease the voltage pulse for a certain amount of induced charges during the thermal neutron detection. That will degrade the detection efficiency. Indeed, deep levels are produced by irradiation then these fixed charges should be measureable. The capacitances of all three devices remain the same as before irradiation as shown in Figure 7, indicating that the neutron detection performance is not degraded. The relatively small capacitance (~ 6 pF at -10 V) of P1 as compared to ~ 100 pF of F1 and D1 is because of its small physical size and the relatively low dielectric constant of photoresist as compared to Boron and Si.

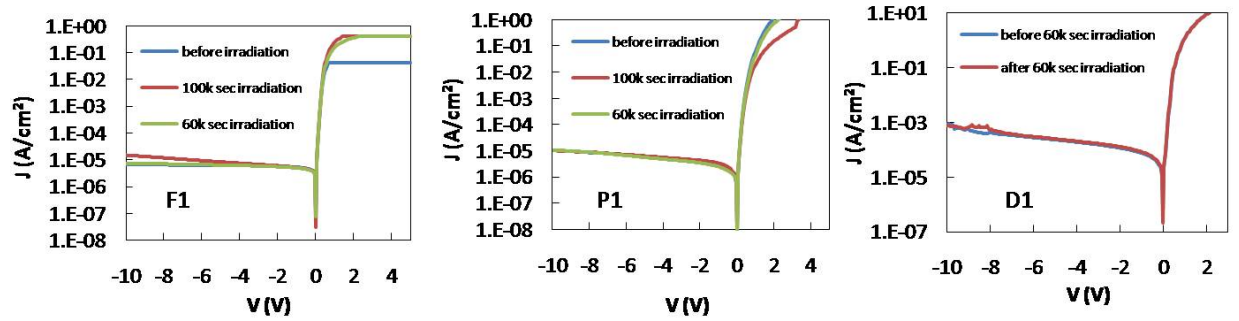

Figure 5 Current-voltage characteristics of F1 (flat), P1 (pillar with photoresist) and D1 (detector: pillar with ^{10}B) before and after gamma irradiation

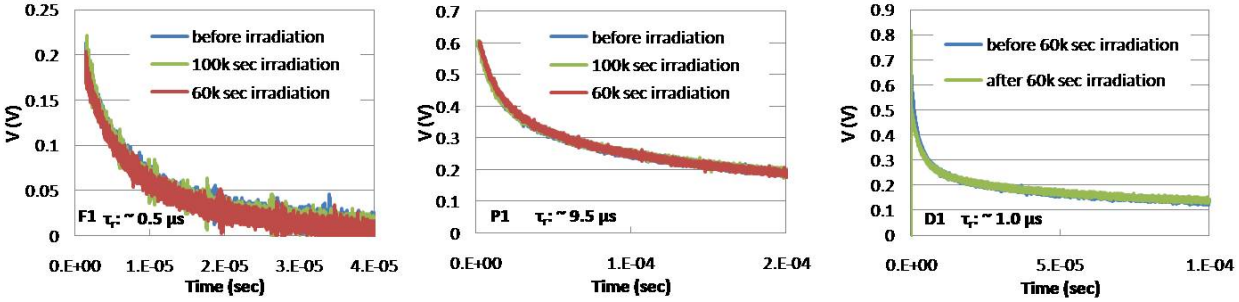

Figure 6 Open-Circuit Voltage Decay (OCVD) waveforms of F1 (flat), P1 (pillar with photoresist) and D1 (detector: pillar with ^{10}B) before and after gamma irradiation.

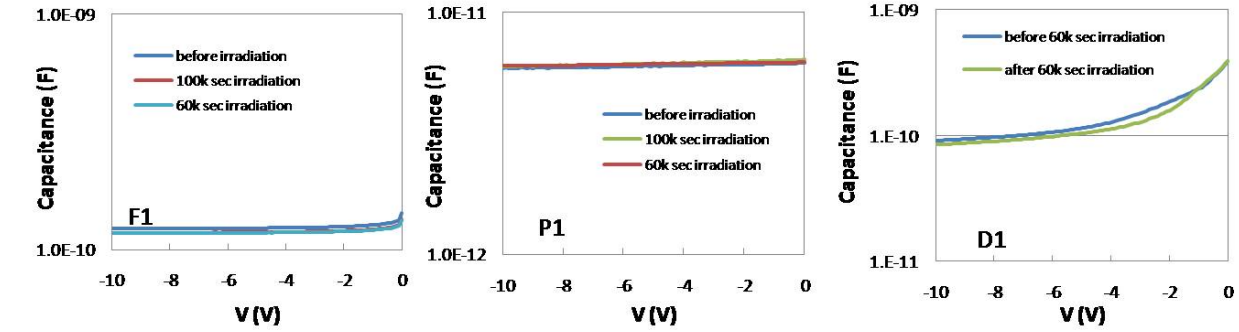

Figure 7 Capacitance-voltage characteristics of F1 (flat), P1 (pillar with photoresist) and D1 (detector: pillar with ^{10}B) before and after gamma irradiation.

2. Device performance after fast neutron irradiation

The electrical measurements (I-V, OCVD and C-V) were taken before and after neutron irradiation on D1. As shown in Figure 8, all electrical properties of the detector (D1) remain same. The neutron response of D1 was measured using a ^{252}Cf neutron source with intensity of 3.85×10^{8} n/sec and moderated by 30 cm in diameter sphere D_2O and covered with 1 mm of Cd

[18]. The measurement time was 60,000 seconds. A 0.5 micro-second shaping time was used. The detector was operated at 0 V during the measurement. Figure 9 shows that there is no appreciable change in terms of total neutron counts after the high fluence gamma and neutron irradiation.

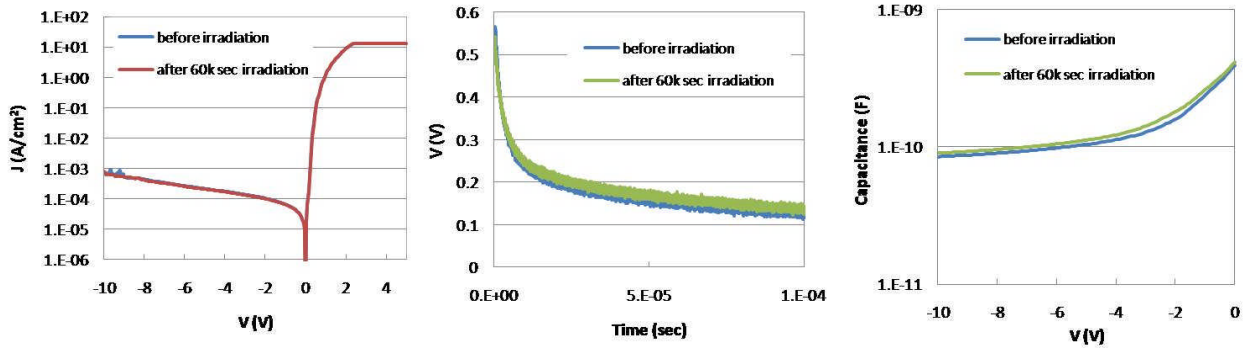

(a) (b) (c)

Figure 8 Current-voltage (a), OCVD (b) and capacitance-voltage (c) characteristics of D1 (detector: pillar with ^{10}B) before and after fast neutron irradiation.

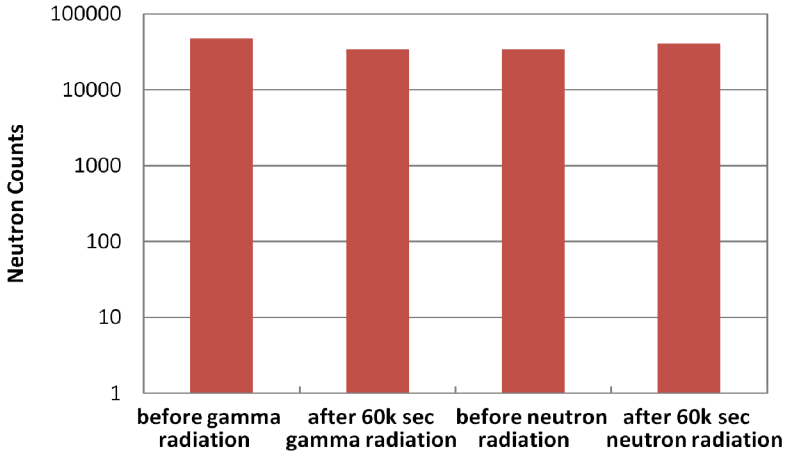

Figure 9 Total neutron counts of D1 before and after high fluence gamma/neutron irradiation.

Degradation of detector performance for planar detectors under irradiation is typically caused by two mechanisms: nonionizing energy loss (NIEL), which causes a change in effective doping concentration, increase of leakage current and an increase in charge trapping, and ionizing energy loss (IEL), which can lead surface damage. NIEL is caused by interactions between neutral particles (neutron and gamma) and the Si portion of the detector directly, while IEL is caused by the neutron - ^{10}B reaction by-products (alpha and Li) interaction with the Si pillars. The change in leakage current due to an increase in space charge generation in Si detectors is given by [19]:

$$\Delta I/V=\alpha\Phi_{eff} \quad (1)$$

, where ΔI is the change in leakage current after irradiation, V is the active volume, α is the damage factor and Φ_{eff} is the 1MeV equivalent neutron fluence. A survey of literature results show that α ranges from $1x10^{-17}$ [20] to $5x10^{-17}$ A/cm [19]. Assuming this theory applies to our

pillar detector at 1×10^{-3} A/cm^2 a Φ_{eff} of $1x10^{16}$ n/cm^2 is needed . For gamma - Si interaction, the damage coefficient is even lower at 1×10^{-23} A/cm [19] requiring a 10^6 higher total fluence for observable degradation than for the neutron fluence.

Further experiments with higher fluencies exposed to three devices need to be performed to determine the effect of irradiation on our pillar detector and evaluate possible failure modalities due to large surface area of the pillars as compared to the flat diode and the robustness of the boron within the pillars as compared to the photoresist filled device.

CONCLUSION

In summary, we have shown that there are no catastrophic device failures for our pillar structured thermal neutron detector when irradiated under high fluence gamma 2.0×10^{14} photons/cm^2 and neutron 1.9×10^8 n/cm^2. This has been confirmed by monitoring the electrical and radiation response of our device after high fluence radiation. Time to failure analysis will need to be done to determine precise failure mechanisms.

ACKNOWLEDGEMENTS

The authors would like to acknowledge Tim Graff and Cathy Reinhardt for their excellent support in cleanroom fabrication and commitment to the LLNL Pillar Project. This work was performed under the auspices of the U.S. Department of Energy by Lawrence Livermore National Laboratory under Contract DE-AC52-07NA27344, LLNL-CONF-434285. This work was supported by the Domestic Nuclear Detection Office in the Department of Homeland Security.

REFERENCES

1. A. M. Conway, R. J. Nikolic and T. F. Wang, "Numerical simulations of carrier transport in pillar structured solid state thermal neutron detector," International Semiconductor Device Research Conference, College Park, MD, December 12-14, 2007.
2. R. J. Nikolic, A. M. Conway, C. E. Reinhardt, R. T. Graff, T. F. Wang, N. Deo and C. L. Cheung, Invited, "Pillar structured thermal neutron detectors," International Conference on Solid State and Integrated Circuit Technology (ICSICT), Beijing, China, October 20-23, 2008.
3. R. J. Nikolic, C. L. Cheung, C. E. Reinhardt and T. F. Wang, "Roadmap for high efficiency solid-state neutron detectors," SPIE - International Symposium on Integrated Optoelectronic Devices, Vol. 6013, no. 1, pp. 36-44 (2005).
4. R. J. Nikolic, A. M. Conway, C. E. Reinhardt, R. T. Graff, T. F. Wang, N. Deo and C. L. Cheung, "Pillar structured thermal neutron detector with 6:1 aspect ratio," Appl. Phys. Lett. 93, 133502 (2008).
5. Q. Shao, A. M. Conway, L. F. Voss, D. P. Heineck, C. E. Reinhardt, R. T. Graff and R. J. Nikolic, "Leakage current quenching and lifetime enhancement in 3D pillar structured silicon PIN diodes," International Semiconductor Device Research Conference, College Park, MD, December 9-11, 2009.

6. A. M. Conway, T. F. Wang, N. Deo, C. L. Cheung and R. J. Nikolic, "Numerical simulations of pillar structured solid state thermal neutron detector: efficiency and gamma discrimination," IEEE Trans. on Nuclear Science, 56, pp. 2802-2807 (2009).
7. Nicholas Tsoulfanidis, "Measurement and detection of radiation," Chapter 7, Hemisphere Publishing Corporation, New York, 1983.
8. Milton Ohring, "Reliability and failure of electronic materials and devices," Chapter 1, Academic Press, 1998.
9. W. Shockley and W.T. Read, "Statistics of the recombination of holes and electrons," Phys. Rev. 87(5), p. 835, (1952).
10. Donald A. Neamen, "An introduction to semiconductor devices," Chapter 9, The McGraw-Hill Companies, Inc. 2006.
11. S. J. Watts, J. Matheson, I. H. Hopkins-Bond, A Holmes-Siedle, A. Mohammadzadeh and R. Pace, "A new model for generation-recombination in silicon depletion regions after neutron irradiation," IEEE Trans. Nuclear Science, 43(6), pp. 2587-2594, (1996).
12. J. Matheson, M. S. Robbins and S. J. Watts, "The effect of radiation induced defects on the performance of high resistivity silicon diodes," RD20 Technical Report CERN RD20/TN/95-36, January (1995).
13. E. Fretwurst, H. Herdan, J. L. Lindstrom, U. Pein, M. Rollwagon, H. Schatz, P. Thomses and R. Wunstorf, "Silicon detector developments for calorimetry, technology and radiation damage," Nuclear Instruments and Methords in Physics Research, A288, pp. 1-12, (1990).
14. G. R. Hopkinson, C. J. Dale and P. W. Marshall, "Proton effects in CCDs," IEEE Trans. Nuclear Sciences, 43(2), pp. 614-627 (1996).
15. J. E. Mahan, T. W. Ekstedt, R. I. Frank and R. Kaplow, "Measurement of minority carrier lifetime in solar cells from photo-induced open-circuit voltage decay," IEEE Trans. Electron Devices, ED-26, No. 5, pp. 733-739 (1979).
16. M. A. Green, "Minority carrier lifetimes using compensated differential open circuit voltage decay," Solid State Electronics, 26 (11), pp. 1117-1122 (1983).
17. M. Tapajna, J. Pjencak, A. Vrbicky, L. Harmatha and P. Kudela, "Applications of open circuit voltage decay to the characterization of epitaxial layer," Journal of Electrical Engineering, 55 (9-10), pp. 239-244 (2004).
18. R. Radev, "Characterization of the neutron fields in the Lawrence Livermore National Laboratory (LLNL) radiation calibration laboratory low scatter calibration facility," LLNL Report LLNL-TR-416791, April, 2009.
19. G. Lindstrom, "Radiation damage in silicon detectors," Nuclear Instruments and Methods in Physics Research A, 512, pp.30-43 (2003).
20. W. Dabrowski, K. Korbel and A. Skoczen, "Fast neutron damage of silicon PIN photodiodes," Nuclear Instruments and Methods in Physics Research A, 301, pp. 288-294 (1991).